

A highly selective chemosensor for nickel(II) based on fluorescence quenching of a bispyrazole derivative

Lu Lin¹ · Sheng-Ting Hu¹ · Yao-Chao Yan¹ ·
Dun-Jia Wang¹ · Ling Fan¹ · Yan-Jun Hu¹ ·
Guo-Dong Yin¹

Received: 14 February 2016 / Accepted: 22 June 2016
© Springer Science+Business Media Dordrecht 2016

Abstract A novel bispyrazole, 2,6-bis(5-phenyl-1*H*-pyrazol-3-yl)-pyridine, was designed and synthesized. The bispyrazole showed extreme selectivity for Ni²⁺ over other metal ions such as Ag⁺, Al³⁺, Ba²⁺, Ca²⁺, Cd²⁺, Co²⁺, Cr³⁺, Cu²⁺, Fe³⁺, Hg²⁺, K⁺, Mg²⁺, Na⁺, Pb²⁺, and Zn²⁺ in MeOH–H₂O solution. The sensing sensitivity and binding properties of the bispyrazole for nickel(II) ion were investigated by fluorescent spectroscopic techniques. It was found that the bispyrazole possessed high selectivity and sensitivity toward Ni²⁺ over other metal ions. The binding stoichiometry was confirmed as 1:1 (bispyrazole/Ni²⁺) by Job plot experiment and the linearity of the Benesi–Hildebrand plot. The binding constants *K* and thermodynamic parameters (ΔH , ΔG , and ΔS) at different temperatures were obtained. Meanwhile, the detection limit of the bispyrazole for Ni²⁺ was determined to be 3.25×10^{-7} mol L⁻¹.

Keywords Nickel(II) · Chemosensor · Fluorescence quenching · Binding constants · Thermodynamic parameters · 2,6-bis(5-Phenyl-1*H*-pyrazol-3-yl)-pyridine

Introduction

Fluorescent chemosensors for heavy- and transition-metal ions have received considerable attention due to their useful applications in environmental sciences, biology, and chemistry [1–3]. In recent years, many highly selective and sensitive fluorescent probes

Electronic supplementary material The online version of this article (doi:[10.1007/s11164-016-2621-9](https://doi.org/10.1007/s11164-016-2621-9)) contains supplementary material, which is available to authorized users.

✉ Dun-Jia Wang
dunjiaawang@163.com

¹ College of Chemistry and Chemical Engineering, Hubei Collaborative Innovation Center for Rare Metal Chemistry, Hubei Key Laboratory of Pollutant Analysis and Reuse Technology, Hubei Normal University, Huangshi 435002, China

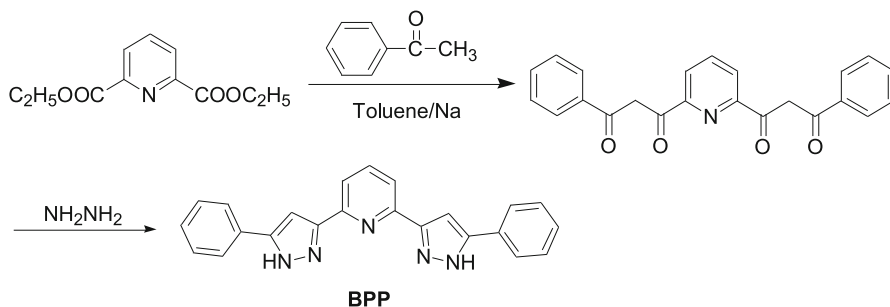
for metal ions have been reported [4–10]. Among these metal ions, nickel(II) ion is an essential micronutrient for animals and plants. Loss of nickel homeostasis is harmful to prokaryotic and eukaryotic organisms [11]. In excess, it can lead to serious problems such as asthma, pneumonitis, respiratory system cancer, and disorders of the central nervous system [12]. Therefore, it is necessary and important to develop an effective method for determining the amount of nickel(II) ion. Conventional analytical methods such as atomic absorption spectrometry, plasma emission spectroscopy, inductively coupled plasma mass spectrometry, and X-ray fluorescence have been used for nickel assay. Most of these approaches are sophisticated and time consuming, not being suitable for quick, online detection. The fluorimetric chemosensor method for detecting nickel is expected to be more desirable because it is relatively easier, cheaper, and highly sensitive. Recently, a few studies have reported determination of nickel(II) ion based on chemical optical sensors. Yari et al. [13] developed a new nickel(II) ion-selective optode based on 2-amino-1-cyclopentene-dithiocarboxylic acid. Gupta et al. [14] reported a nickel(II)-selective sensor based on dibenzo-18-crown-6 in a poly(vinyl chloride) (PVC) matrix. Aksuner et al. [15] reported a novel optical chemical sensor for determination of nickel(II) based on fluorescence quenching.

In this study, we designed a new bispyrazole derivative, 2,6-bis(5-phenyl-1*H*-pyrazol-3-yl)-pyridine (BPP), to act as a fluorescent chemosensor for metal ion detection. The chemosensor BPP was synthesized by condensation of the corresponding bis- β -diketone with hydrazine hydrate (Scheme 1). The metal ions Ag^+ , Al^{3+} , Ba^{2+} , Ca^{2+} , Cd^{2+} , Co^{2+} , Cr^{3+} , Cu^{2+} , Fe^{3+} , Hg^{2+} , K^+ , Mg^{2+} , Na^+ , Ni^{2+} , Pb^{2+} , and Zn^{2+} were tested for metal ion binding selectivity using the chemosensor BPP. Fortunately, nickel(II) ion exhibited strong fluorescent quenching upon binding with the chemosensor BPP. Thus, the chemosensor BPP can be used as an excellent sensor for detecting nickel(II) ions.

Experimental

Materials and instrumentation

Acetophenone, diethyl 2,6-pyridinedicarboxylate, sodium, hydrazine hydrate, and 4-(2-hydroxyethyl)-1-piperazineethanesulfonic acid (HEPES) were purchased from



Scheme 1 Synthesis of bispyrazole BPP

Sun Chemical Technology (Shanghai) Co., Ltd. Other reagents used were of analytical grade and were used without further purification.

Melting points were measured on an X-4 digital melting point apparatus and are uncorrected. Elemental analysis (C, H, N) was determined on a PerkinElmer 2400 elemental analyzer. Infrared (IR) spectra were recorded on a Nicolet FTIR 5700 spectrophotometer with KBr pellets. ^1H nuclear magnetic resonance (NMR) spectra were measured on an Advance IIITM 300 MHz NB digital NMR spectrometer in dimethyl sulfoxide (DMSO)- d_6 solution with tetramethylsilane (TMS) as internal standard. Electrospray ionization mass spectra (ESI-MS) were obtained with a Finnigan LCQ advantage max spectrometer. Ultraviolet–visible (UV–Vis) spectra were obtained on a Hitachi U-3010 spectrometer. Fluorescence emission spectra were obtained with a Varian Cary Eclipse fluorescence spectrometer. pH measurements were carried out using a PHS-3C pH-meter (Shanghai, China).

Synthesis of 2,6-bis(5-phenyl-1H-pyrazol-3-yl)pyridine (BPP)

The bis- β -diketone, 3,3'-pyridin-2,6-diyl-bis(1-phenylpropane-1,3-dione), was prepared by Claisen condensation of diethyl 2,6-pyridinedicarboxylate with acetophenone in toluene using sodium as condensing agent according to literature [16].

3,3'-Pyridin-2,6-diyl-bis(1-phenylpropane-1,3-dione) (0.28 g, 0.75 mmol) was dissolved in chloroform (30.0 mL), and hydrazine hydrate (0.32 g, 6.4 mmol) was added dropwise under stirring. The reaction mixture was refluxed for 1 h. Then the solvent was removed, and white precipitate was obtained. The crude products were recrystallized from absolute ethanol to give the bispyrazole (BPP) as pale crystals. Yield 75 %, m.p. 162–163 °C; IR (KBr): ν 3432(s), 3199(s), 3021(m), 1568(s), 1457(s), 1284(m), 1180(m), 1078(m), 1052(m), 961(m), 803(s), 763(s) cm^{-1} ; ^1H NMR (300 MHz, DMSO- d_6): δ 13.60 (bs, 2H, NH), 7.94–7.82 (m, 5H, Ar-H), 7.83 (d, J = 7.6 Hz, 2H, Ar-H), 7.53 (s, 2H, C = CH), 7.49–7.44 (m, 4H, Ar-H), 7.35 (t, J = 7.2 Hz, 2H, Ar-H) ppm; ESI-MS m/z : 364.39 $[\text{M} + 1]^+$; Anal. calcd. for $\text{C}_{23}\text{H}_{17}\text{N}_5$: C 76.01, H 4.71, N 19.27; found C 76.42; H 4.69; N 19.36; UV–Vis (CHCl_3): λ = 264 nm (ϵ = 23,225 $\text{L mol}^{-1} \text{cm}^{-1}$), 312 nm (ϵ = 9325 $\text{L mol}^{-1} \text{cm}^{-1}$) (a figure showing the UV–Vis results for BPP is provided in the Electronic Supplementary Material).

Procedures for metal ion sensing

Stock solution of bispyrazole BPP (1.0×10^{-3} mol/L) was prepared in methanol. Stock solution for metal ions was prepared in 1:1 (v/v) MeOH– H_2O solution with concentration of 1.0×10^{-3} mol/L. HEPES buffer solution (1.0×10^{-2} mol/L, pH 7.0) was prepared using HEPES and sodium hydroxide. Working solution of BPP (1.0×10^{-5} mol/L) was prepared in methanol by adding HEPES buffer solution to adjust the pH to 7.0.

In the experiments, 3.0 mL solution of BPP (1.0×10^{-5} mol/L) was placed in a quartz cell (1 cm width), and the solution of metal ions was added into the quartz cell gradually by microsyringe to obtain the working solution. The volume for the solution of metal ions added was $<75 \mu\text{L}$ to prevent noticeable change of the total

volume of the testing solution. Fluorescence emission spectra of BPP were recorded in the λ_{em} range of 300–500 nm at $\lambda_{\text{ex}} = 258$ nm with 5.0/5.0 nm slit width and 500 V photomultiplier tube (PMT) voltage.

Results and discussion

Metal ion sensing properties

The sensing ability of the chemosensor (BPP) for various metal ions was investigated by adding tenfold molar excess of metal ions (Ag^+ , Al^{3+} , Ba^{2+} , Ca^{2+} , Cd^{2+} , Co^{2+} , Cr^{3+} , Cu^{2+} , Fe^{3+} , Hg^{2+} , K^+ , Mg^{2+} , Na^+ , Ni^{2+} , Pb^{2+} , and Zn^{2+}) into BPP, a neutral 10:1 (v/v) MeOH–H₂O solution. The changes in the fluorescence spectrum of BPP upon addition of different metal ions are presented in Fig. 1. It was observed that the fluorescence intensity of BPP showed negligible variation in the presence of Ag^+ , Al^{3+} , Ba^{2+} , Ca^{2+} , Co^{2+} , Cr^{3+} , Fe^{3+} , K^+ , Mg^{2+} , and Na^+ . However, metal ions Cd^{2+} , Cu^{2+} , Hg^{2+} , Pb^{2+} , and Zn^{2+} caused fluorescence quenching to some extent. Interestingly, nickel(II) ion revealed very distinct quenching activity over other metal ions, as it could quench the fluorescence of BPP completely. For practical applicability, competitive experiments of the chemosensor BPP for Ni^{2+} ion were carried out. The changes in the fluorescence intensity for BPP were determined on treatment with 10 equiv. Ni^{2+} ion in the presence of the same equiv. of other metal ions (Fig. 2). From Fig. 2, all of the tested interfering metal ions showed no observable interference with the detection of Ni^{2+} ion. Therefore, bispyrazole BPP can be used as a highly selective chemosensor for nickel(II) ion. In addition, the pH value had a great influence on the detection procedure. We determined the fluorescence intensity of BPP in absence and presence of nickel(II) ion in the pH range from 3.0 to 10.0 (Fig. 3). From Fig. 3, the fluorescence OFF–ON system worked well in the pH range from 6.5 to 7.5 in 10:1 (v/v) MeOH–H₂O solution. Acidic medium (pH < 6.5) caused decreased emission intensity, probably due to a weakened conjugate system by formation of BPP ammonium salt. At higher pH values (pH > 7.5), BPP competed with OH^- ion for Ni^{2+} ion, increasing metal ion precipitation and accordingly weakening the fluorescence quenching effect.

To elicit the chemosensing properties of BPP toward nickel(II) ion, fluorescence titrations with Ni^{2+} in 10:1 (v/v) MeOH–H₂O were carried out at two different temperatures (288 and 298 K). In absence of nickel(II) ion, the fluorescence maximum of BPP (10 μM) was centered at about 356 nm and its fluorescence intensity was strongest. As shown in Fig. 4, upon gradual addition of Ni^{2+} (0.52–5.24 μM), the fluorescence intensity gradually decreased with increasing Ni^{2+} concentration, forming the basis for fluorimetric determination of nickel(II) ion. In addition, when ethylenediaminetetraacetic acid (EDTA, 0–7.0 μM) was added to BPP– Ni^{2+} solution, the fluorescent intensity at 356 nm was gradually enhanced due to chelation of Ni^{2+} ion with EDTA, releasing the chemosensor BPP (Fig. 5). These results indicate that BPP could be developed as a reversible fluorescence chemosensor for Ni^{2+} ion.

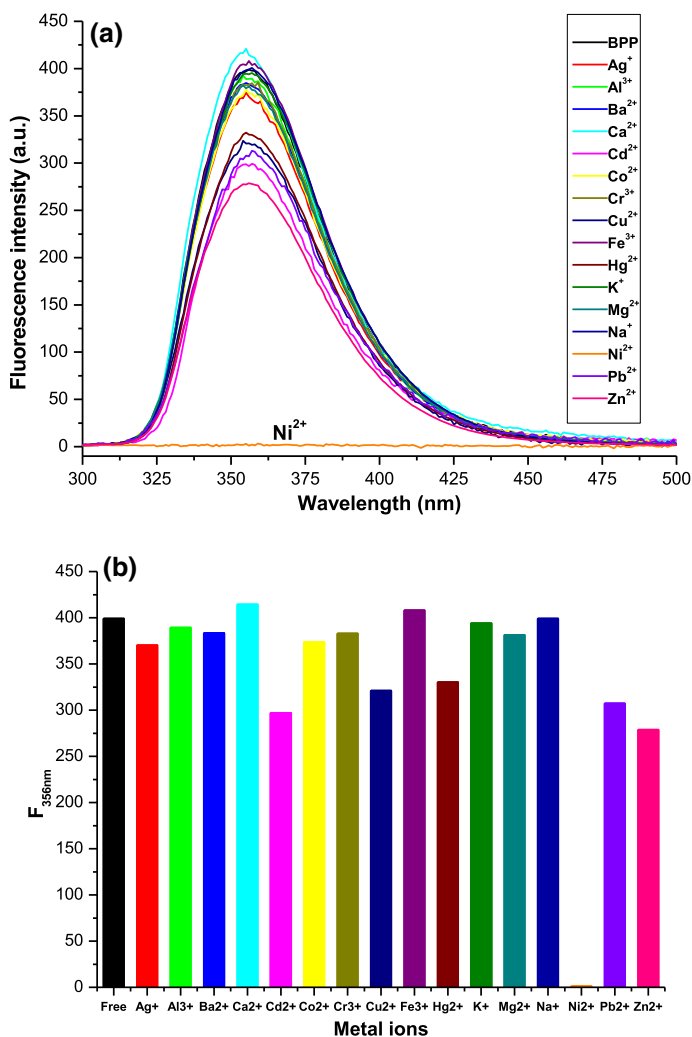


Fig. 1 **a** Fluorescence spectra of BPP (10 μM) upon addition of different metal ions (0.1 mM) in 10:1 (v/v) MeOH–H₂O (pH 7.0) solution. **b** Histogram of fluorescence selectivity experiment ($\lambda_{\text{ex}} = 258 \text{ nm}$)

Fluorescence quenching data are presented as plots of F_0/F versus $[Q]$ at different temperatures (288 and 298 K) in Fig. 6. These results show that this quenching process is in agreement with the Stern–Volmer equation [17],

$$F_0/F = 1 + K_{\text{SV}}[Q], \quad (1)$$

where F_0 and F are the fluorescence intensities in absence and presence of quencher, respectively, K_{SV} is the dynamic quenching constant, and $[Q]$ is the concentration of quencher.

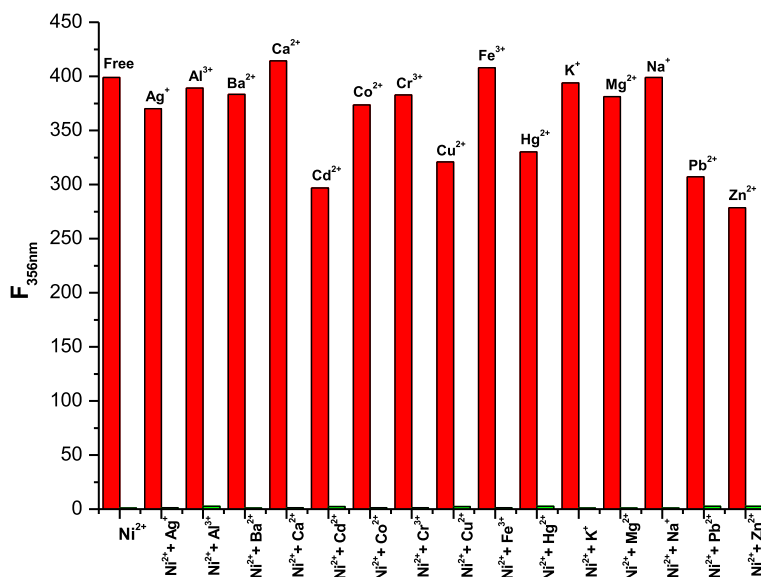


Fig. 2 Competitive selectivity of BPP (10 μM) in 10:1 (v/v) MeOH–H₂O (pH 7.0) solution toward Ni^{2+} (10 equiv.) in presence of other metal ions (10 equiv.) with excitation at 258 nm

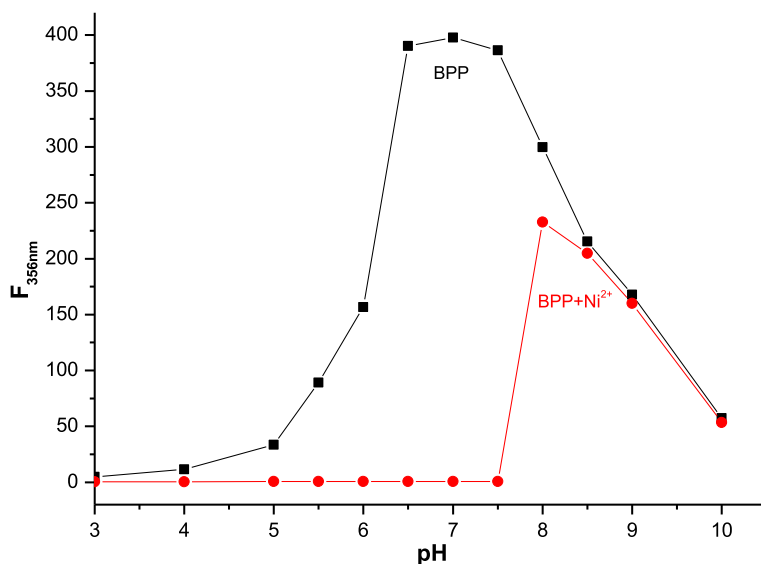


Fig. 3 Fluorescence intensity of BPP at various pH values in absence and presence of Ni^{2+} (5.0 equiv.) at $\lambda_{\text{em}} = 356 \text{ nm}$

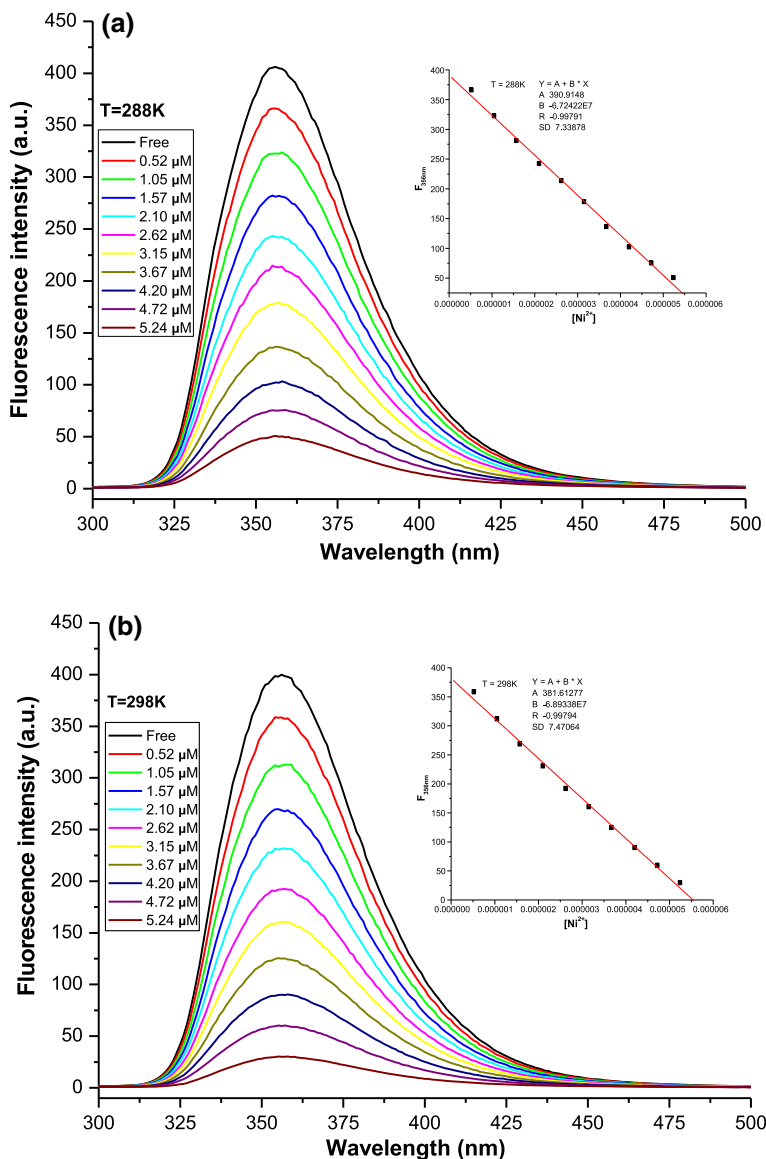


Fig. 4 Fluorescence spectra of BPP (10 μM) in 10:1 (v/v) MeOH–H₂O (pH 7.0) solution upon addition of different concentrations of Ni²⁺ (0.52–5.24 μM) at two different temperatures (**a** $T = 288$ K, **b** $T = 298$ K). The insets show the emission intensity at $\lambda_{em} = 356$ nm as a function of [Ni²⁺] ($\lambda_{ex} = 258$ nm)

The dynamic quenching constants (K_{SV}) calculated for the interaction between BPP and Ni²⁺ were 5.73×10^5 ($R = 0.9900$) at 288 K and 4.75×10^5 ($R = 0.9911$) at 298 K. Evidently, K_{SV} decreased with increasing temperature. It

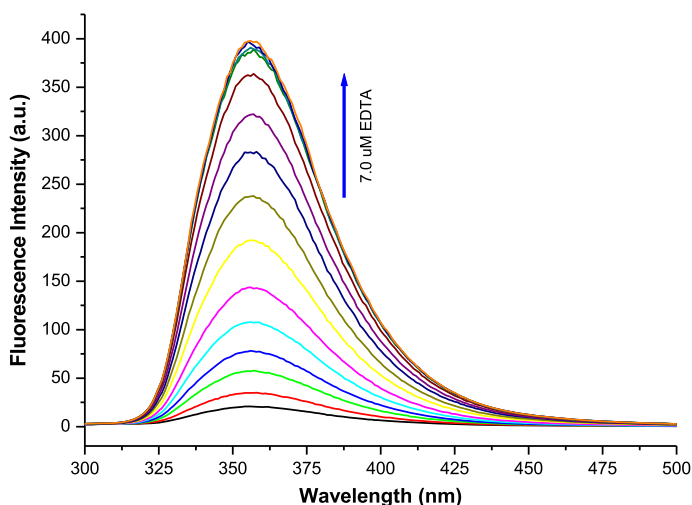


Fig. 5 Changes in fluorescence spectrum of BPP–Ni²⁺ in 10:1 (v/v) MeOH–H₂O (pH 7.0) solution upon gradual addition of EDTA (0–7.0 μM) ($\lambda_{\text{ex}} = 258 \text{ nm}$)

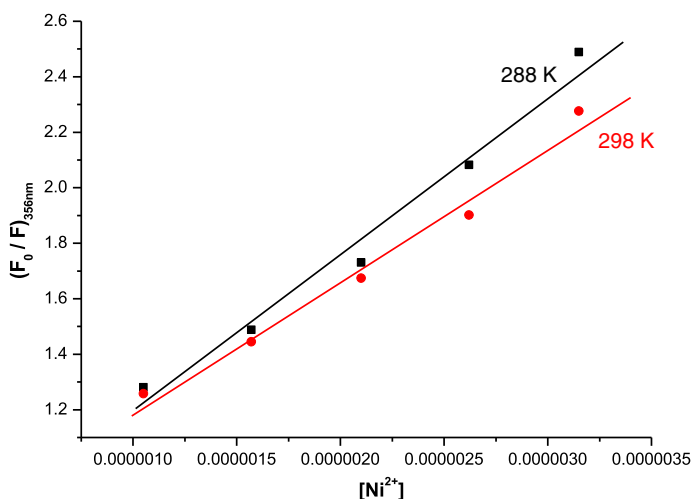


Fig. 6 Stern–Volmer plots for quenching between BPP and Ni²⁺ at 288 and 298 K

can be concluded that the interaction between BPP and the Ni²⁺ quencher can probably be described by a static quenching model [18].

The binding stoichiometry of the chemosensor BPP–Ni²⁺ complex was also deduced based on Job plot experiments [19]. The fluorescence intensity at 356 nm was plotted against the molar fraction of nickel(II) ion under a constant total concentration of BPP and Ni²⁺ in 10:1 (v/v) MeOH–H₂O solution. Maximum

fluorescent quenching occurred when the mole fraction of nickel(II) ion was close to 0.5 (Fig. 7), indicating a 1:1 stoichiometric ratio between BPP and nickel(II) ion.

Binding constants and detection limit

The binding constants for the chemosensor BPP–Ni²⁺ complex were determined by the Benesi–Hildebrand equation [20],

$$\frac{1}{F - F_0} = \frac{1}{F_{\max} - F_0} + \frac{1}{(F_{\max} - F_0)K[\text{Ni}^{2+}]^n}, \quad (2)$$

where [Ni²⁺] is the nickel(II) ion concentration, F is the fluorescence intensity at 356 nm for given Ni²⁺ concentration, F_0 is the fluorescence intensity at 356 nm in absence of Ni²⁺, and F_{\max} is the maximum fluorescence intensity at 356 nm in presence of Ni²⁺ in solution. The binding constant K is determined from the ratio of the intercept and slope of the Benesi–Hildebrand plot. If the plot of $1/[F - F_0]$ versus $1/[\text{Ni}^{2+}]$ ($n = 1$) gives a straight line, then the complex stoichiometry is 1:1, whereas if the plot of $1/[F - F_0]$ versus $1/[\text{Ni}^{2+}]^2$ ($n = 2$) gives a straight line, then the stoichiometry of the complex between chemosensor BPP and nickel(II) ion will be 1:2.

Analysis of the fluorescence titration curves at two different temperatures (Fig. 3) by Benesi–Hildebrand plots (Fig. 8) revealed that plots of $1/(F - F_0)$ versus $1/[\text{Ni}^{2+}]$ were both a straight line, indicating a 1:1 complex between BPP and nickel(II) ion. These results are in good agreement with the corresponding values obtained from the molar ratio method. On the basis of plots of $1/(F - F_0)$ versus

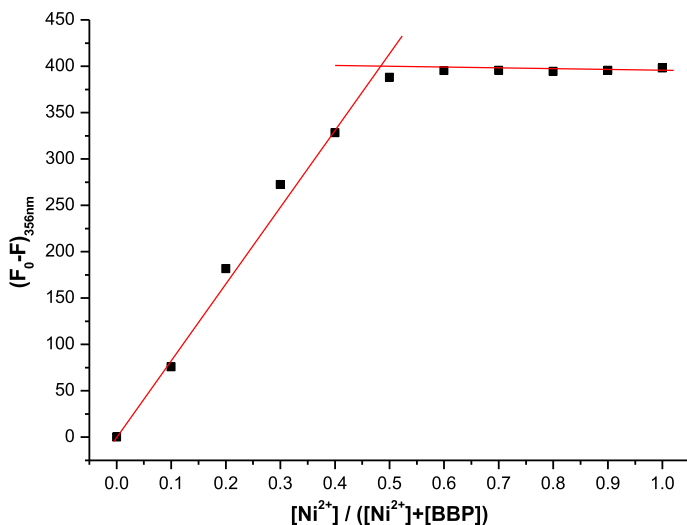


Fig. 7 Job plot of 1:1 complex between BPP and Ni²⁺, where the 356-nm emission is plotted against mole fraction of Ni²⁺ under constant total concentration of 10 μM in 10:1 (v/v) MeOH–H₂O (pH 7.0) solution

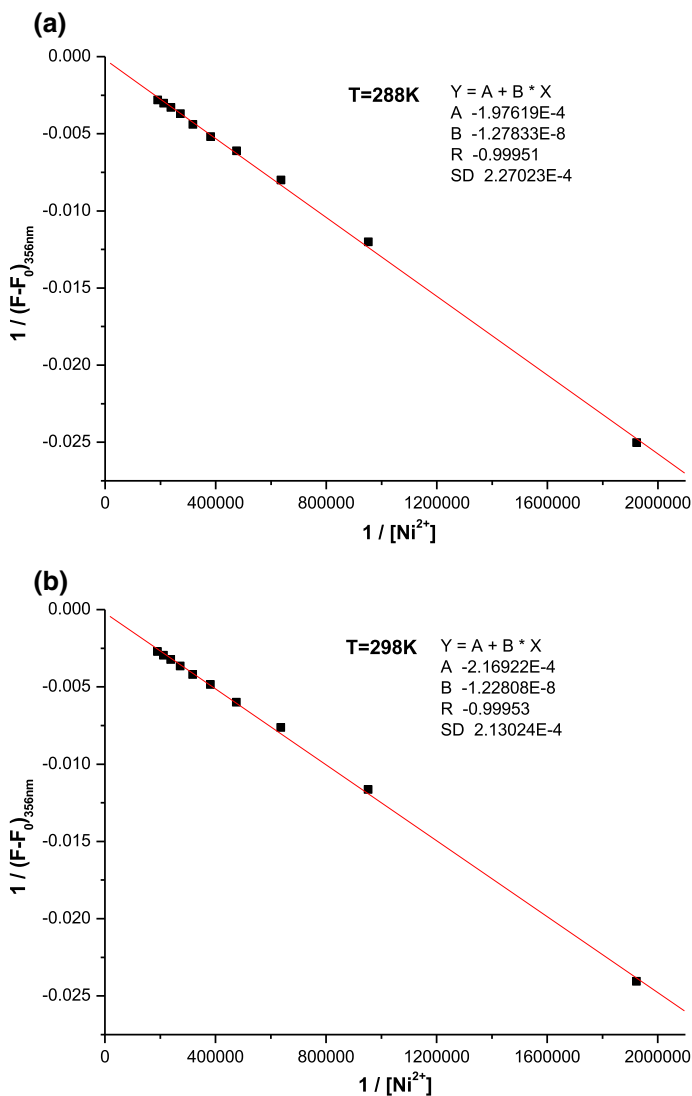
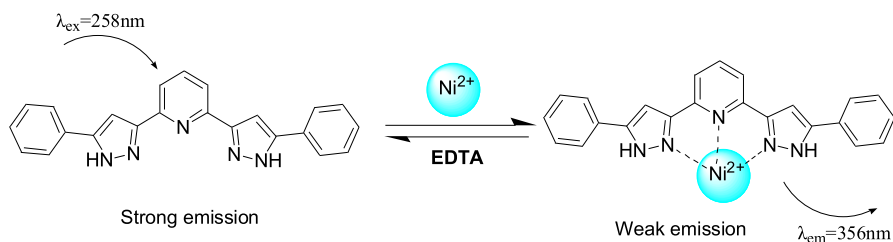


Fig. 8 Benesi-Hildebrand plots of BPP with Ni^{2+} at two different temperatures (**a** $T = 288$ K, **b** $T = 298$ K). The excitation wavelength was 258 nm, and the monitored emission wavelength was 356 nm

$1/[\text{Ni}^{2+}]$ (Fig. 4), the binding constants at 288 and 298 K were calculated to be $1.55 \times 10^4 \text{ M}^{-1}$ ($R = 0.99951$) and $1.77 \times 10^4 \text{ M}^{-1}$ ($R = 0.99953$), respectively.

According to the above results, the bispyrazole BPP could be used as a reversible fluorescence chemosensor for Ni^{2+} ion. The possible binding mode between BPP and Ni^{2+} ion is presented in Scheme 2.

To obtain the detection limit of Ni^{2+} ion using the chemosensor BPP, BPP ($10 \mu\text{M}$) was treated with various concentrations of Ni^{2+} (0.52 – $5.24 \mu\text{M}$). At room



Scheme 2 Proposed binding mode between BPP and Ni^{2+}

temperature, the fluorescence intensity at 356 nm was plotted as a function of Ni^{2+} concentration. As shown in Fig. 9, the fluorescence intensity of BPP was linearly proportional to the Ni^{2+} concentration in the range of 0.52–5.24 μM . The linear regression equation was determined to be $F_0 - F = 18.25 + 6.89 \times 10^7 [\text{Ni}^{2+}]$ ($n = 9$, $R = 0.99794$, $\text{SD} = 7.47064$). The detection limit was determined from the following equation [21, 22]: detection limit = $3 \times \text{SD}/B$, where SD is the standard deviation of blank measurement and B is the slope of the fluorescence intensity versus the Ni^{2+} concentration. The calculated detection limit for Ni^{2+} ion was 3.25×10^{-7} M, which is sufficiently low to enable detection of micromolar amounts of nickel(II) ion.

Thermodynamic parameters

To further elucidate the interaction between BPP and nickel(II) ion, the thermodynamic parameters were determined according to the Van't Hoff equations (3–5) [23, 24]. The enthalpy change (ΔH) can be regarded as a constant if the temperature

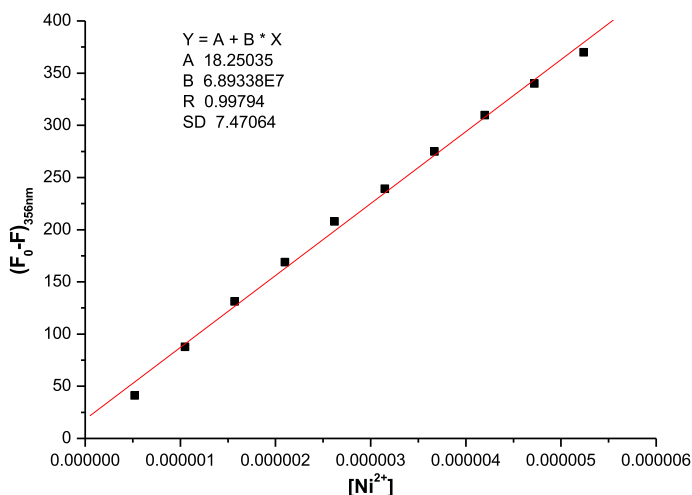


Fig. 9 Fluorescence intensity ($F_0 - F$) versus Ni^{2+} concentration at room temperature. The excitation wavelength was 258 nm, and the monitored emission wavelength was 356 nm

Table 1 Binding constants and thermodynamic parameters of BPP with Ni²⁺

<i>T</i> (K)	<i>K</i> (M ⁻¹)	ΔG (kJ mol ⁻¹)	ΔS (J mol ⁻¹ K ⁻¹)	ΔH (kJ mol ⁻¹)
288	1.55×10^4	-23.10	113.21	9.51
0298	1.77×10^4	-24.23	113.22	

does not vary significantly. The free energy change (ΔG) can be calculated from Eq. (3) based on the binding constants at different temperatures (288 and 298 K).

$$\Delta G = -RT \ln K, \quad (3)$$

where R is the gas constant, T is the experimental temperature, and K is the binding constant at the corresponding temperature. Then, the enthalpy change (ΔH) and entropy change (ΔS) can also be obtained from the following equations:

$$\ln \frac{K_2}{K_1} = \left(\frac{1}{T_1} - \frac{1}{T_2} \right) \frac{\Delta H}{R}, \quad (4)$$

$$\Delta G = \Delta H - T\Delta S. \quad (5)$$

The calculated values of the thermodynamic parameters (ΔH , ΔG , and ΔS) are listed in Table 1. Among these thermodynamic parameters, the negative ΔG value implies that the interaction process between BPP and nickel(II) ion is spontaneous [25]. The positive ΔH value indicates that their interaction is an endothermic process, and the positive ΔS value also reveals the chelating characteristic of the chemosensor BPP with nickel(II) ion [26].

Conclusions

A new chemosensor, 2,6-BPP, was synthesized and characterized by Fourier-transform infrared (FTIR), ¹H NMR, elemental analysis, and mass spectrometry. The sensing selectivity and sensitivity, and binding properties of BPP for nickel(II) ion were investigated in neutral 10:1 (v/v) MeOH–H₂O solution. The chemosensor BPP exhibited high selectivity and sensitivity toward Ni²⁺ over other metal ions. The fluorescence emission of BPP could be effectively quenched upon addition of Ni²⁺ (0.52–5.24 μM) in MeOH–H₂O solution, and the corresponding quenching process can probably be described by a static quenching model. The binding ratio of BPP and Ni²⁺ was determined to be 1:1, as confirmed by Job plot experiment and the linearity of the Benesi–Hildebrand plot. The binding constants K and thermodynamic parameters (ΔH , ΔG , and ΔS) were also calculated, and the detection limit of BPP for Ni²⁺ was found to be 3.25×10^{-7} mol L⁻¹. Thus, bispyrazole BPP can be used as a highly selective, sensitive, and reversible chemosensor for sensing micromolar concentrations of nickel(II) ion.

Acknowledgments We gratefully acknowledge financial support from the National Natural Science Foundation of China (nos. 21542009 and 21273065) and the Educational Commission of Hubei Province (no. B2015132).

References

1. H. Hisamoto, K. Suzuki, *Trends Anal. Chem.* **18**, 513–524 (1999)
2. K. Rurack, *Spectrochim. Acta Part A* **57**, 2161–2195 (2001)
3. M. Beija, C.A.M. Afonso, J.M.G. Martinho, *Chem. Soc. Rev.* **38**, 2410–2433 (2009)
4. J. Ding, L. Yuan, L. Gao, J. Chen, *J. Lumin.* **132**, 1987–1993 (2012)
5. D. Zhang, Y. Ma, R. An, *Res. Chem. Intermed.* **41**, 5059–5069 (2015)
6. Z.-J. Jiang, H.-S. Lv, J. Zhu, B.-X. Zhao, *Synth. Met.* **162**, 2112–2116 (2012)
7. D. Şahin, H. Yılmaz, Z. Hayvalı, *Res. Chem. Intermed.* (2016). doi:[10.1007/s11164-016-2466-2](https://doi.org/10.1007/s11164-016-2466-2)
8. R. Senthilnithy, M.D.P. De Costa, H.D. Gunawardhana, *Luminescence* **24**, 203–208 (2008)
9. L. Feng, Z. Chen, D. Wang, *Spectrochim. Acta Part A* **66**, 599–603 (2007)
10. S. Goswami, S. Chakraborty, A.K. Das, A. Manna, A. Bhattacharyya, C.K. Quah, H.-K. Fun, *RSC Adv.* **4**, 20922–20926 (2014)
11. A. Sigel, H. Sigel, R.K.O. Sigel, *Nickel and Its Surprising Impact in Nature*, vol. 2 (Wiley, London, 2007)
12. S.C. Dodani, Q. He, C.J. Chang, *J. Am. Chem. Soc.* **131**, 18020–18025 (2009)
13. A. Yari, M.B. Gholivand, F. Rahhedayat, *Measurement* **44**, 1691–1698 (2011)
14. V.K. Gupta, R.N. Goyal, S. Agarwal, P. Kumar, N. Bachheti, *Talanta* **71**, 795–800 (2007)
15. N. Aksuner, E. Henden, I. Yilmaz, A. Cukurovali, *Sens. Actuators B* **166–167**, 269–274 (2012)
16. H. Liu, J.H. Yang, L. Lin, D.J. Wang, L. Fan, Y.J. Hu, *Res. Chem. Intermed.* **42**, 2857–2866 (2016)
17. D.-J. Gao, Y. Tian, S.-Y. Bi, Y.-H. Chen, A.-M. Yu, H.-Q. Zhang, *Spectrochim. Acta Part A Mol. Biomol. Spectrosc.* **62**, 1203–1208 (2005)
18. M.D.P. De Costa, W.A.P.A. Jayasinghe, *J. Photochem. Photobiol. A Chem.* **162**, 591–598 (2004)
19. A. Senthilvelan, I. Ho, K. Chang, G. Lee, Y. Liu, W. Chung, *Chem. Eur. J.* **15**, 6152–6160 (2009)
20. H. Benesi, J.H. Hildebrand, *J. Am. Chem. Soc.* **71**, 2703–2707 (1949)
21. B.P. Joshi, J. Park, W.I. Lee, K.H. Lee, *Talanta* **78**, 903–909 (2009)
22. S.R. Liu, S.P. Wu, *J. Fluoresc.* **21**, 1599–1605 (2011)
23. S.Y. Bi, D.Q. Song, Y.H. Kan, D. Xu, Y. Tian, *Spectrochim. Acta Part A* **62**, 203–212 (2005)
24. J. Jayabharathi, V. Thanikachalam, R. Sathishkumar, K. Jayamoorthy, *J. Photochem. Photobiol. B* **117**, 222–227 (2012)
25. C. Wang, Q.H. Wu, C.R. Li, Z. Wang, J.J. Ma, X.H. Zang, N.X. Qin, *Anal. Sci.* **23**, 429–433 (2007)
26. K.S. Siddiqi, S. Bano, A. Mohd, A.A.P. Khan, *Chin. J. Chem.* **27**, 1755–1761 (2009)